2017

Protocols and pitfalls in obtaining fatty acid-binding proteins for biophysical studies of ligand-protein and protein-protein interactions

Qian Wang
CUNY Graduate Center

Samar Rizk
CUNY Graduate Center

Cédric Bernard
CUNY City College

May Poh Lai
CUNY Graduate Center

David Kam
CUNY City College

See next page for additional authors

Authors

Qian Wang, Samar Rizk, Cédric Bernard, May Poh Lai, David Kam, Judith Storch, and Ruth E. Stark

Protocols and pitfalls in obtaining fatty acid-binding proteins for biophysical studies of ligand-protein and protein-protein interactions

Qian Wang[a,b,c,1], Samar Rizk[a,b,c,1], Cédric Bernard[a,c], May Poh Lai[a,b,c], David Kam[a,c], Judith Storch[d], Ruth E. Stark[a,b,c,e,f,g,*]

[a] Department of Chemistry and Biochemistry, The City College of New York, New York, NY 10031, USA
[b] Ph.D. Program in Biochemistry, The Graduate Center of the City University of New York, New York, NY 10016, USA
[c] CUNY Institute for Macromolecular Assemblies, New York, NY 10031, USA
[d] Department of Nutritional Sciences, School of Environmental and Biological Sciences, Rutgers University, New Brunswick, NJ 08901, USA
[e] Ph.D. Program in Chemistry, The Graduate Center of the City University of New York, New York, NY 10016, USA
[f] Ph.D. Program in Physics, The Graduate Center of the City University of New York, New York, NY 10016, USA
[g] Ph.D. Program in Biology, The Graduate Center of the City University of New York, New York, NY 10016, USA

ARTICLE INFO

ABSTRACT

Adipocyte fatty acid-binding protein (AFABP: FABP4) is a member of the intracellular lipid-binding protein family that is thought to target long-chain fatty acids to nuclear receptors such as peroxisome proliferator-activated receptor gamma (PPARγ), which in turn plays roles in insulin resistance and obesity. A molecular understanding of AFABP function requires robust isolation of the protein in liganded and free forms as well as characterization of its oligomerization state(s) under physiological conditions. We report development of a protocol to optimize the production of members of this protein family in pure form, including removal of their bound lipids by mixing with hydrophobically functionalized hydroxypropyl dextran beads and validation by two-dimensional NMR spectroscopy. The formation of self-associated or covalently bonded protein dimers was evaluated critically using gel filtration chromatography, revealing conditions that promote or prevent formation of disulfide-linked homodimers. The resulting scheme provides a solid foundation for future investigations of AFABP interactions with key ligand and protein partners involved in lipid metabolism.

1. Introduction

Fatty acid-binding proteins (FABPs) are low molecular weight (~15 kDa) members of the intracellular lipid-binding protein (iLBP) family with 20–70% sequence identity [1] and the ability to bind both long-chain fatty acids (LCFA) and other hydrophobic ligands reversibly. Functional studies implicate FABPs in trafficking and targeting of LCFAs to the nucleus, where their interactions with *e.g.* the peroxisome proliferator-activated receptors (PPARs) have been demonstrated both in vitro and for hepatocyte cells [2–5]. Some FABPs exhibit a nuclear localization signal in their three-dimensional fold; when activated by particular ligands, translocation of the FABP from the cytosol to the nucleus and delivery of the ligand to its PPAR partner are promoted [6,7]. Together these proteins play important roles in signal transduc-

tion, cell growth, cell cycle and differentiation [8]; the action of adipose FABP, for instance, has been linked to hyperglycemia, insulin resistance, and obesity [9]. In addition, some reports have correlated the circulating level of adipocyte FABP (AFABP; FABP4) to the development of Type-2 diabetes [9,10]. While typically considered to exist as monomers, several FABPs appear to have a tendency to self-associate [7,11].

To define the molecular mechanisms underlying AFABP function, it is first essential to isolate and characterize the protein under near-physiological conditions. An ideal preparative method should be efficient and reproducible; it should yield an unliganded (apo) FABP that retains its native solution-state fold and oligomerization state without rapid deterioration; it should be amenable to probing with respect to three-dimensional conformation and binding to ligands or

other protein partners. These goals can be elusive even for the small soluble iLBPs, due to the affinity of FABPs for the *E. coli* cellular constituents associated with their expression and/or the reported tendency of a few family members to form dimers or multimers [7,11,12].

This Report outlines protocols that optimize the production of AFABP and can be extended to other members of this large protein family. A newly developed scheme is presented to obtain efficient expression and purification, also achieving removal of bound lipids and/or fatty acids with validation made by two-dimensional NMR spectroscopy. We define conditions that promote or prevent formation of AFABP homodimers, either by self-association or covalent bonding though disulfide bridges. These procedures provide a macromolecular entity that is suitable for subsequent molecular-level studies of protein-ligand and protein-protein interactions, both of which are involved in metabolic signaling in mammalian tissues.

2. Materials and methods

2.1. Molecular cloning, expression, and purification of recombinant AFABP

Scheme S1 and the accompanying commentary describe cloning of the murine AFABP DNA including an N-terminal His$_6$-tag and a Tobacco Etch Virus (TEV) protease cleavage site, protein overexpression in *E. coli* cells and purification using HistidineTrap and gel filtration chromatography.

2.2. Delipidation of AFABP

Hydrophobic materials that are bound tightly to AFABP such as endogenous lipids generated during *E. coli* growth were removed from association with the protein via preferential binding to a Lipidex-5000 resin [13] (Sigma, H6383) which consisted of a lipophilic Sephadex LH–20–100 (hydroxypropyl beaded dextran) that was substituted with C13–C18 alkyl ethers. In our implementation of this strategy, a 5-gram portion of dry beads was activated by immersing in 5 mL of gel filtration (GF) buffer (described in the Supplementary information), then shaking in a conical Falcon tube at 37 °C for 2.5 h. To the resulting suspension was added 40–45 mL of protein solution (50 mg of protein), followed by shaking at 225 rpm and 37 °C for 2 h; no packed columns were used. The beads were removed using a 0.22-μm Millipore Amicon filter (Mahopac, NY). Two cycles of this treatment were carried out to ensure completeness of the delipidation. Similar procedures were followed for the intestinal and liver-type FABPs.

2.3. Isolation and development of apo-AFABP oligomers

To verify the oligomerization state of the AFABP protein, a prepacked XK26/40 column of Superdex 75 (GE Healthcare) was used for gel filtration chromatography. Protein samples, diluted serially from 460 to 11.5 μM, were injected and eluted with GF buffer at a flow rate of 0.6 mL/min on XK26/40 for large loading amounts (20 mL) or 0.25 mL/min on a Superdex 75 10/300 column for small loading amounts (100 μL). Molecular weight calibration used a protein standard kit spanning the range of 6.5 – 75 kDa; Blue Dextran (2000 kDa) served to determine the column void volume. Elution profiles were monitored for volumes of 0–25 mL using the Absorbance at 280 nm. Relative areas of monomer (lagging) and dimer (leading) fractions were determined in triplicate for each sample by calculating the respective peak areas. To test for disulfide linkages in the oligomers recovered from GF, standard SDS-PAGE was compared with gels run in the presence of 25% β-mercaptoethanol that can break such bonds.

The role of exposure to oxygen gas in the formation of putative disulfide-bonded AFABP dimers was examined by monitoring the dimer proportion as a function of time. The recovered monomer (lagging) fraction from GF of freshly prepared AFABP was split into two portions.

One portion was treated with oxygen-free nitrogen gas, which was passed through a reservoir containing 100 mM vanadium sulfate, 25 mL sulfuric acid and 10 g zinc metal for one hour; the protein sample was then sealed with a rubber cap and Parafilm. The second portion was left with the cap open to the air. Both samples were maintained at 4 °C for a total time period of one month, including collection and testing of aliquots by GF at roughly one-week intervals. The dimer proportion was calculated by calculating the peak areas as a function of development time.

2.4. Mass spectrometry

Electrospray Ionization Mass Spectrometry (ESI-MS) was performed on a Bruker Maxis II ETD instrument (Bruker Biospin, Billerica, MA). Samples were exchanged with 200 mM ammonium acetate by using 10 kDa Amicon Ultra-15 filters, then concentrated to 10 μM before injection into the mass spectrometer at 3 μL/min. Typical native ESI-MS runs used a source temperature of 150 °C, dry nitrogen gas kept at 4 L/min, and a collision cell voltage optimized to 5 V. Matrix-assisted laser desorption/ionization time-of-flight mass spectrometry (MALDI-TOF) was conducted with a Bruker Autoflex Speed-High-Performance System using protein samples concentrated to 10 μM and mixed at 1:1 (v/v) with 10 mg/mL of a sinapic acid matrix.

2.5. Solution-state NMR spectroscopy

The two- and three-dimensional NMR experiments [14] were performed at 20 °C on a Bruker Avance I spectrometer operating at 500 MHz and equipped with a 5-mm TXI cryoprobe (Bruker Biospin, Billerica, MA). The AFABP sample (400 μM, assuming all proteins are monomers) was prepared in a solution that contained 10% (v/v) D$_2$O, 10 mM potassium phosphate, 150 mM potassium chloride and 0.2 g/L sodium azide, adjusted to pH 7.4. The 2D ^{1}H–^{15}N heteronuclear single quantum correlation (HSQC) spectra were acquired with respective spectral widths of 14 ppm and 32 ppm in the ^{1}H and ^{15}N dimensions, requiring 8–128 scans (0.7–11 h) in separate experiments at a range of protein concentrations. For 2D nuclear Overhauser and total correlation spectroscopy (^{1}H–^{15}N NOESY-HSQC and ^{1}H–^{15}N TOCSY-HSQC) experiments, the typical mixing and spin-lock times were 150 ms and 70 ms, respectively. The triple-resonance experiments (HNCO, HN(CA)CO, HNCACB and CBCA(CO)NH) were conducted using typical acquisition and processing parameters described previously [15,16]. The resulting data were processed using NMRPipe software [17] and analyzed by NMRViewJ software [18].

3. Results and discussion

3.1. Apo-AFABP purification has been optimized and validated

Following the protocol outlined in Section 2, recombinant murine AFABP was overexpressed in *E. coli* and purified to obtain ~30 mg protein per liter of LB culture (unlabeled samples) or ~25 mg per liter of minimal media (^{15}N- or ^{15}N,^{13}C-enriched protein samples for NMR spectroscopy). After sequential purification by affinity and size exclusion chromatography, TEV protease cleavage conducted with expedited removal of the linker yielded a protein of the expected 15 kDa molar mass that was verified to have excellent purity by both SDS-PAGE and MALDI-TOF MS methods (Fig. 1). As compared with prior purifications of FABPs [16,19], this method required half the time of schemes using size exclusion and ion exchange chromatography while maintaining a robust overall yield of ≥25 mg for a 1-L culture.

Prior publications on related members of the FABP family, including several reports from our own laboratories, have described the removal of bound lipids by column chromatography with Lipidex-1000 beads (hydroxyalkoxypropyl Sephadex), hydrophobic interaction column chromatography (phenyl Sepharose), or acidic precipitation. Such
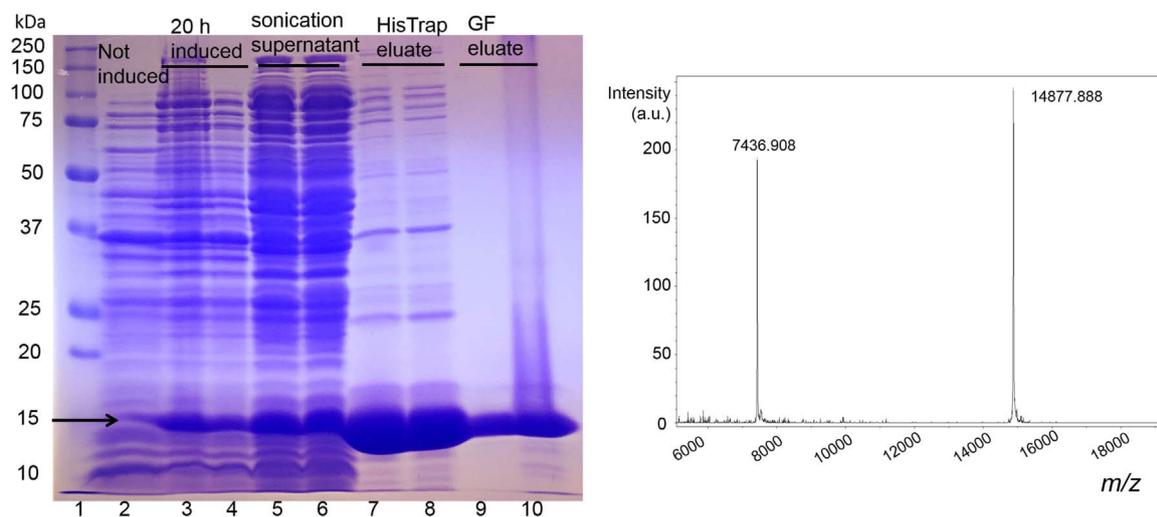
Fig. 1. Chromatographic purification of murine adipose fatty acid-binding protein (mAFABP) monitored by SDS-PAGE and verified by MALDI-TOF MS. *Left:* Lane 1, protein marker ladder, with an arrow showing the mass of AFABP; lane 2, culture before induction with L-arabinose; lanes 3 and 4, 20-h induced samples, omitting and including β-mercaptoethanol (BME) treatment to check for disulfide bridges; lanes 5 and 6, lysis supernatant after sonication, omitting and including BME; lanes 7 and 8, HisTrap eluate, omitting and including BME; lanes 9 and 10, gel filtration eluate, omitting and including BME. *Right:* The MALDI-MS data for these (undelipidated) samples exhibit two major peaks corresponding to doubly and singly charged molecular ions, respectively.

protocols were designed to remove either endogenous cellular materials in the *E. coli* culture or ³H-oleate added to ensure protein folding and to monitor the purification [15,19–22]. Some studies of AFABP ligand binding have omitted the delipidation step from the purification altogether, with the premise that tightly binding ligands will displace any residual cellular lipids [7,23].

In prior solution-state structural studies of FABPs, the two-dimensional ¹H–¹⁵N HSQC NMR spectra displayed an environmentally distinct amide resonance for each backbone polypeptide residue, except for missing signals corresponding typically to a few prolines and the 10% flexible loop sites that underwent intermediate NH exchange on the NMR timescale [15,24,25]. However, after Lipidex-1000 chromatography we observed ~35% more AFABP signals than anticipated. Many of the weaker resonances appeared at chemical shifts corresponding to lipid-bound AFABP (Fig. 2, **left**), indicating that the standard delipidation method was insufficient. Retention of fatty acids by ~50% of human AFABP after

diverse Lipidex treatments has also been reported using solution-state NMR and X-ray crystallography (PDB: 2HNX) [26]. Analogous purifications for the liver-type and intestinal proteins of this family with currently available Lipidex-1000 materials also showed incomplete delipidation by NMR (Fig. S1; S. Sarkar, personal communication).

To improve the completeness of AFABP delipidation, we developed a scheme to optimize the chromatographic matrix and improve the contact between protein and Lipidex materials. Lipidex-5000 beads were used to provide a more hydrophobic resin, the beads were suspended in buffer in a conical tube, and the protein solution was mixed directly at a high bead-to-protein ratio that promoted lipid removal. After two mixing cycles we incurred losses of ~20%. Distinct apo- and holo-AFABP resonances were observed in the undelipidated NMR spectra rather than a single peak located at a position corresponding to a weighted average of the two protein populations, consistent with tight lipid binding and slow exchange of polypeptide amide groups on the NMR timescale. Comparisons of two-
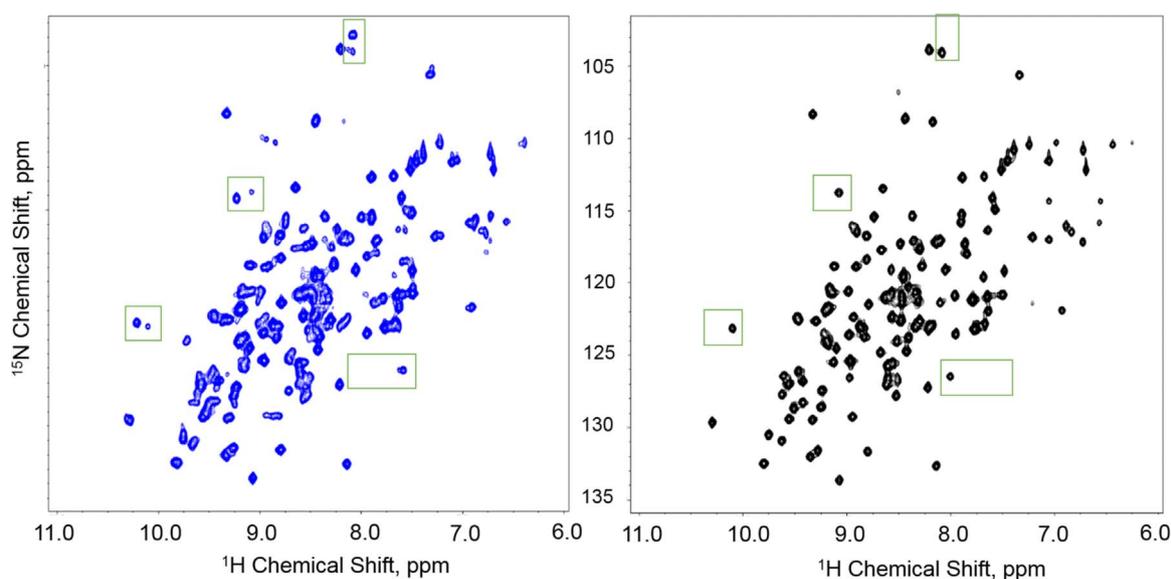

Fig. 2. NMR contour plots of results from ¹H–¹⁵N HSQC experiments [4] conducted on 200 μM adipose fatty acid-binding protein samples at a ¹H frequency of 500 MHz. Chemical shifts are referenced according to the guidelines of Wishart et al. [28]. A comparison of the un-delipidated spectrum (left, blue) and the twice-delipidated spectrum (right, black) includes green boxed regions to highlight differences between the unliganded [22] protein state and a mixture of holo and apo states. (For interpretation of the references to color in this figure legend, the reader is referred to the web version of this article.)
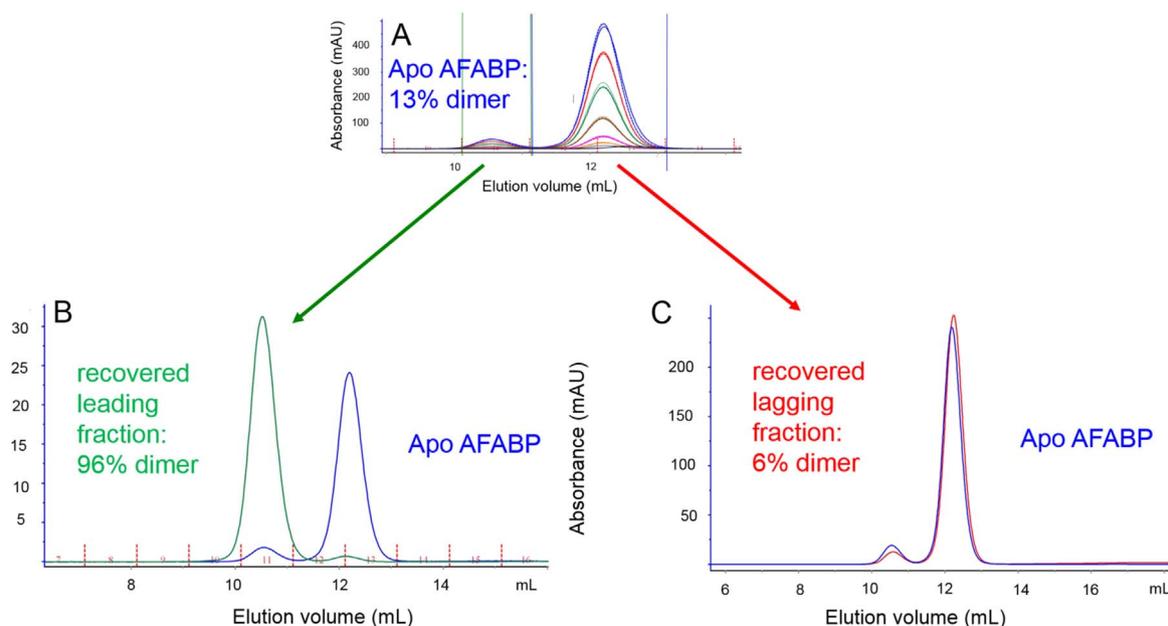
Fig. 3. Elution profiles for murine adipose fatty acid-binding protein obtained from size exclusion chromatography (gel filtration with Superdex 75). A: Dilution series (462 μM; royal blue to 11.5 μM; navy blue) of twice-delipidated apo-AFABP samples stored for one month at 4 °C and analyzed in triplicate, showing reproducible dimer percentages within 1% for each sample and a nearly invariant dimer percentage (13.3 ± 0.3%) throughout the indicated 50-fold concentration range. B: Recovered leading fraction (green) and original 15.2 ± 5.6 μM apo-protein elution shown in panel A (blue). C: Recovered lagging fraction (red) and original 231.0 ± 0.8 μM apo-protein from the elution shown in panel A (blue). Each trace in panels B and C represents an average of three GF chromatograms. (For interpretation of the references to color in this figure legend, the reader is referred to the web version of this article).

dimensional ^{1}H–^{15}N HSQC NMR spectra were made for un-delipidated, once-delipidated and twice-delipidated protein samples, where Fig. 2 shows that the holo-AFABP peak intensities (left spectrum) decreased after one cycle of delipidation (not shown) and were nearly unobservable after two cycles (right spectrum) (< 3% estimated by comparing signals to the noise level in one-dimensional spectral slices). Native ESI-MS was also used to confirm the presence of ~55% oleate-bound AFABP in preparations to which a twofold excess of ligand had been added to stabilize the protein after cell lysis and the absence of the holo protein after two cycles of swirling with Lipidex-5000. The difference of mass between 8 + -charged ions appearing at m/z 1895.7977 and 1860.4012 was used to verify the expected molecular weight of 282 g/mol for this bound species. Thus the suspended-bead protocol described above yielded more complete lipid removal than column chromatography – with either hydrophobic interaction chromatography or Lipidex-5000 media. Analogous procedures were also used successfully for liver-type and intestinal FABPs (Fig. S1).

These results provided a validated means to obtain apo-AFABP and permitted straightforward determination of sequence-specific NMR resonance assignments. Although backbone amide assignments were available for human AFABP, which displays 92% sequence similarity with the murine AFABP studied herein [25], fewer than 30% of the chemical shift assignments could be transferred directly. Nonetheless, it was possible to observe 94% of the expected backbone and side chain NH resonances and to assign 90% of the backbone NH residues site-specifically (deposited to the BioMagResBank under accession number 27096). Standard protocols of double-resonance (^{1}H–^{15}N-NOESY-HSQC and ^{1}H–^{15}N-TOCSY-HSQC) and triple-resonance experiments (HNCO, HN(CA)CO, HNCACB and CBCA(CO)NH) were used for [U-^{15}N]-labeled and [U-^{13}C,^{15}N]-labeled proteins, respectively [27,28]. Together with augmented delipidation, these spectroscopic assignments laid the groundwork for studies of both molecular affinity and interaction loci of the fatty acid-binding protein with respect to physiologically important ligand and protein partners by NMR and calorimetric methods.

3.2. AFABP monomers can be separated from a minor dimer form

Although it has been widely assumed that FABPs are present in monomeric form, at the near-physiological concentrations used for

thermodynamic and NMR studies of their interactions with ligands and other proteins, non-covalently associated dimers were proposed by Gillilan et al. [7]. Such associated species would not be evident in the SDS-PAGE gels of Fig. 1 and could conceivably be missed in the 2D HSQC NMR spectra of Fig. 2 due to the modest molecular weight of this protein. To establish the oligomeric state of the apo-AFABP sample, a series of protein samples at concentrations from ~10 to ~500 μM were analyzed by gel filtration size exclusion chromatography (GF), typically after refrigerated storage for up to 25 days. The resulting elution profiles, which are overlaid in Fig. 3A, each displayed two well-separated peaks from protein species that differed in molecular size, as deduced from their respective retention volumes. Reference to calibration standards showed that the leading and lagging peaks correspond to approximate molar masses of 32 kDa (an AFABP dimer) and 16 kDa (the monomer). Each profile showed the lagging peak to be predominant; integration yielded a nearly invariant dimer proportion of 13 ± 0.3% over this 50-fold concentration range. Moreover, GF trials with 2:1 holo-AFABP liganded to oleate, linoleate, or troglitazone (a member of the thiazolidinediones antidiabetic drug family) revealed comparable monomer percentages: 99 ± 1%, 95 ± 5%, and 91 ± 1%, respectively, for dilution series from 500 to 10 μM [29].

The trend in GF-based relative populations reported above would be anomalous if non-covalent association of AFABP molecules established a monomer-dimer equilibrium, as proposed in related protein samples under different experimental conditions based on crystallographic, fluorescence, and small-angle light scattering evidence [7]. In that type of dimer, the predominant monomer proportion should indicate weak binding affinity; then as the sample is diluted, the dimer proportion should decrease to a vanishingly small value rather than remaining constant. Conversely, if the AFABP dimer is linked by one or more covalent bonds, then it is possible to account for the observed constancy of the dimer proportion as a function of overall protein concentration.

In order to test this latter proposal, the leading and lagging fractions from the GF column were each recovered and subjected to another round of size exclusion chromatography. In the case of a non-covalent interaction, the leading and lagging fractions should each re-establish the identical monomer-dimer equilibrium state that would be reflected in the subsequent GF elution profile. Otherwise, there should be a greater dimer proportion observed from the recovered leading fraction
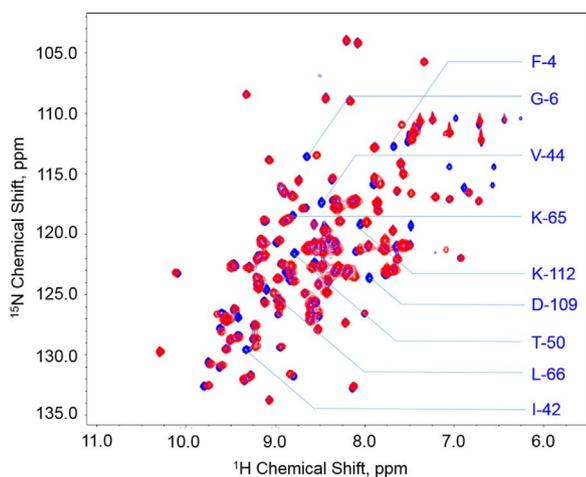
Fig. 4. 500 MHz $^1H–^{15}N$ HSQC NMR [32] contour plot showing overlaid spectra for the recovered monomer (blue, 400 μM) and dimer (red, 200 μM) fractions from GF chromatography of AFABP protein samples. Chemical shifts are referenced according to the guidelines of Wishart et al. [33]. Highly perturbed residues are labeled in the spectrum; a complete plot of chemical shift perturbation as a function of protein sequence appears in Fig. S4. (For interpretation of the references to color in this figure legend, the reader is referred to the web version of this article).

and a lesser proportion from the corresponding lagging fraction, respectively. Figs. 3**B and** 3**C** show GF profiles that illustrate the larger relative amount of dimer in the recovered leading fraction compared to the recovered lagging fraction. This trend argues strongly for an AFABP dimer that is held together (irreversibly) by covalent bond(s). The hypothesis of a leading GF fraction in which a stable dimer predominates was also confirmed using ESI-MS (Fig. S2).

3.3. The AFABP dimer is linked by disulfide bond(s)

Given the common observation of disulfide bonds in proteins [30] and the presence of two surface-accessible cysteine residues in AFABP [26], we hypothesize that our dimer is covalently linked in this fashion. This supposition was tested by monitoring the protein mass in the presence or absence of a β-mercaptoethanol disulfide bond reductant. The SDS-PAGE gels of Fig. S3 showed a dimer band that disappeared upon treatment with a β-mercaptoethanol (BME) reductant. The retention of the 29-kDa band in the absence of BME suggests that the dimer is covalently bound rather than self-associated; its disappearance in the presence of BME supports identification of the AFABP covalent bond as a disulfide linkage. Interestingly, only monomers were
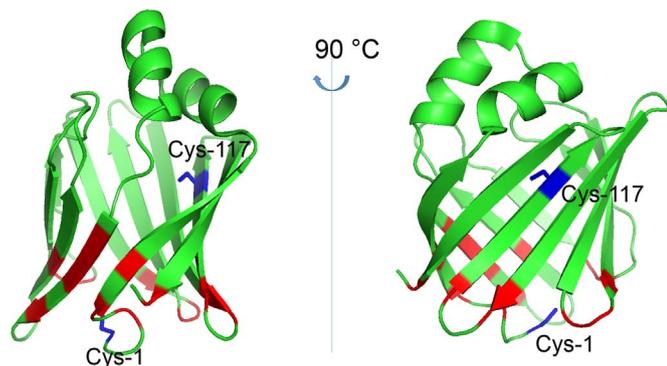
observed from the initial GF conducted during purification and in the recovered lagging fraction samples isolated directly after GF elution, but the dimer proportions grew to ~13% and ~16%, respectively, during refrigerated storage for one month.

3.4. The AFABP dimer forms through an N-terminal cysteine residue

Either of the two cysteine residues within the AFABP protein is a candidate for dimer formation via a disulfide bond, though the N-terminal Cys-1 is expected to have a somewhat more surface-accessible location than Cys-117. In order to verify the location, the recovered AFABP monomer and dimer fractions were each examined using 2D $^1H–^{15}N$ HSQC NMR. The overlaid spectra of Fig. 4 reveal differences in chemical shift for several peaks, *i.e.,* significant perturbations in magnetic environment for the backbone amide groups in particular molecular regions. Sites for which the weighted ^1H and ^{15}N perturbations [31] exceeded one standard deviation beyond the mean value (Fig. S4) were mapped onto the crystal structure of the protein (PDB: 2Q9S) [7]. Fig. 5 shows that the most perturbed region of AFABP is located at the N-terminus, close to the location of Cys-1. These NMR results support the formation of a disulfide bond through the cysteine residue at the N-terminus of the protein sequence.

3.5. AFABP dimer formation can be blocked by excluding oxygen gas

Given that disulfide bond formation is an energy-requiring oxidative process, we hypothesized that oxygen gas dissolved in the phosphate buffer solution could effect this chemical transformation. Formation of inter- or intramolecular S-S bridges under oxidative stress conditions has been established, for instance, in a protein kinase and a protein-tyrosine phosphatase, respectively [34,35]. To test our proposal, a month-long course of dimer development was monitored for freshly purified apo-AFABP samples in a standard oxygen-saturated buffer vs. a buffer infused with oxygen-scrubbed nitrogen gas. The samples were collected at 8–10 day intervals and analyzed by GF to assess their respective dimer proportions (Fig. 6). During the initial week of the time course the dimer population grew commensurately in the two samples. Subsequently, dimer growth progressed linearly in the standard buffer but was essentially halted in the oxygen-free buffer medium. After thirty-five days, the comparative dimer proportions were 19% (oxygen-saturated control) and 5.5% (oxygen-free). (The estimated value after 25 days is 11%, in reasonable agreement with the 13% reported in Fig. 3.) These results support the premise that dissolved oxygen gas is the reactant responsible for formation of the disulfide bond in the AFABP dimer.
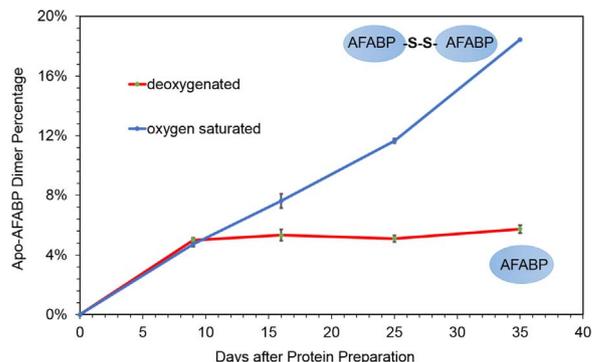

Fig. 5. Mapping of significant chemical shift perturbations on structures depicted with PyMOL [www.pymol.org] for the AFABP dimer with respect to the corresponding protein monomer (PDB: 2Q9S) [7]. Backbone residues highlighted in red exhibit composite $^1H–^{15}N$ NMR chemical shift perturbations of at least one standard deviation beyond the mean value observed for 131 sites of the polypeptide. The cysteine residues that could form disulfide bonds are highlighted in blue. (For interpretation of the references to color in this figure legend, the reader is referred to the web version of this article).

Fig. 6. Proportion of dimers present as a function of time for 56.3 μM (assuming all proteins are monomers) freshly prepared AFABP samples that were stored in buffers saturated with oxygen (blue curve) or infused with oxygen-scrubbed nitrogen gas (red curve). Percentages were derived from elution profiles of Superdex 75 size exclusion gel filtration chromatography analogous to those illustrated in Fig. 3. Error bars denote results from triplicate GF runs on the same sample. (For interpretation of the references to color in this figure legend, the reader is referred to the web version of this article).

4. Context and conclusions

Molecular structural studies at near-physiological concentrations can offer insights and generate hypotheses regarding protein function. For AFABP, these include sequestration of hydrophobic fatty acid metabolic products and transfer of fatty acids to protein binding partners in the nucleus (e.g., PPARγ and JAK2) to effect metabolic signaling [8,9]. Such studies require well-defined protein-ligand and protein-protein systems of high purity, underscoring the importance of robust production and rigorous biophysical characterization. For members of the FABP family, it can be challenging to fulfill the latter requirement in light of tight ligand binding and possible dimerization.

We have developed an efficient purification scheme that provides ≥ 20 mg of ^{15}N-labeled protein from a liter of bacterial culture in minimal media, matching average yields of 15 mg (LFABP) and 25 mg (IFABP) in rich media with traditional FABP isolation procedures while achieving time savings of a factor of two [2,15,16]. This protocol includes robust delipidation that removes > 97% of fatty acids that can have reported K_d values as low as 10 nM [36], keeps losses to a manageable 20% after two removal cycles, avoids the use of radioactive tracers, and can be cross-validated by solution-state NMR.

In contrast to a prior proposal of dimer-driven AFABP activation of nuclear localization that effects metabolic regulation associated with the PPARγ receptor [7], the current measurements did not reveal self-association of AFABP in the manner mentioned in these reports. These divergent results are likely to reflect both crystal packing effects that can produce dimers and differences in respective sample history. For instance, retention of an N-terminal His-tag by Gillilan, *et al.* could preclude disulfide bond formation at Cys-1 while permitting the dimer formation evidenced in fluorescence titrations and small-angle X-ray scattering experiments. The possible retention of endogenous lipids in these and other published studies could also impact both protein interactions with hydrophobic ligands and associated conformational changes.

Nonetheless, oligomerization state is a potentially important consideration with respect to AFABP activation, making it essential to recognize and control the formation of aggregates, including both non-covalently associated and disulfide-linked dimers. Dimers of the type observed herein could also be formed by other FABPs for which the Cys-1 residue is conserved; examples include bacterial, fruit fly, poultry, and fish homologs but no other mammalian FABPs [37–40]. S-S linkages in this protein family have been reported in two instances: for rat cutaneous FABP (FABP5), which has six cysteine residues and forms an intramolecular disulfide linkage (but no dimers), putatively by a red-ox mechanism [41]; and for human heart FABP (FABP3), where dimerization secondary to an intermolecular S-S bond was found [11]. Given the proposed involvement of helix-loop-helix residues in ligand binding and nuclear localization of these proteins [7], dimer formation through the N-termini could conceivably occur without impacting the affinity of FABPs for ligands or nuclear receptors. To avoid the unwitting formation of disulfide-linked protein dimers in AFABP solutions, a protocol of buffer degassing during the purification steps, exclusion of oxygen, and/or addition of reducing agents such as TCEP is recommended. The protocols reported herein lay the groundwork for future investigation of the conformational basis of AFABP interactions with contrasting ligands and proteins such as PPARγ, RAR, and JAK2 that are involved in lipid signaling.

Acknowledgements

Appendix A. Supporting information

Supplementary data associated with this article can be found in the online version at http://dx.doi.org/10.1016/j.bbrep.2017.05.001.

Appendix B. Transparency document

Transparency document associated with this article can be found in the online version at http://dx.doi.org/10.1016/j.bbrep.2017.05.001.

References

[1] S. Chuang, T. Velkov, J. Horne, J. Wielens, D.K. Chalmers, C.J. Porter, M.J. Scanlon, Probing the fibrate binding specificity of rat liver fatty acid binding protein, J. Med. Chem. 52 (2009) 5344–5355.
[2] C. Wolfrum, Lipid sensing and lipid sensors, Cell. Mol. Life Sci. 64 (2007) 2465–2476.
[3] B.R. Thompson, A.M. Mazurkiewicz-Muñoz, J. Suttles, C. Carter-Su, D.A. Bernlohr, Interaction of adipocyte fatty acid-binding protein (AFABP) and Jak2 AFABP/AP2 as a regulator of Jak2 signaling, J. Biol. Chem. 284 (2009) 13473–13480.
[4] N.S. Tan, N.S. Shaw, N. Vinckenbosch, P. Liu, R. Yasmin, B. Desvergne, W. Wahli, N. Noy, Selective cooperation between fatty acid binding proteins and peroxisome proliferator-activated receptors in regulating transcription, Sci. Signal. 22 (2002) 5114.
[5] H.A. Hostetler, A.L. McIntosh, B.P. Atshaves, S.M. Storey, H.R. Payne, A.B. Kier, F. Schroeder, L-FABP directly interacts with PPARα in cultured primary hepatocytes, J. Lipid Res. 50 (2009) 1663–1675.
[6] G. Ohlsson, J.M. Moreira, P. Gromov, G. Sauter, J.E. Celis, Loss of expression of the adipocyte-type fatty acid-binding protein (A-FABP) is associated with progression of human urothelial carcinomas, Mol. Cell. Proteom. 4 (2005) 570–581.
[7] R.E. Gillilan, S.D. Ayers, N. Noy, Structural basis for activation of fatty acid-binding protein 4, J. Mol. Biol. 372 (2007) 1246–1260.
[8] G.S. Hotamisligil, R.S. Johnson, R.J. Distel, R. Ellis, Uncoupling of obesity from insulin resistance through a targeted mutation in aP2, the adipocyte fatty acid binding protein, Science 274 (1996) 1377.
[9] K.T. Uysal, L. Scheja, S.M. Wiesbrock, S. Bonner-Weir, Gk.S. Hotamisligil, Improved glucose and lipid metabolism in genetically obese mice lacking aP2, Endocrinology 141 (2000) 3388–3396.
[10] A.W. Tso, A. Xu, P.C. Sham, N.M. Wat, Y. Wang, C.H. Fong, B.M. Cheung, E.D. Janus, K.S. Lam, Serum adipocyte fatty acid–binding protein as a new biomarker predicting the development of type 2 diabetes A 10-year prospective study in a Chinese cohort, Diabetes Care 30 (2007) 2667–2672.
[11] S.U. Nielsen, H. Vorum, F. Spener, R. Brodersen, Two-dimensional electrophoresis of the fatty acid binding protein from human heart: evidence for a thiol group which can form an intermolecular disulfide bond, Electrophoresis 11 (1990) 870–877.
[12] J.R. Thompson, J.M. Bratt, L.J. Banaszak, Crystal structure of cellular retinoic acid binding protein I shows increased access to the binding cavity due to formation of an intermolecular β-sheet, J. Mol. Biol. 252 (1995) 433–446.
[13] D. Apter, O. Jänne, R. Vihko, Lipidex chromatography in the radioimmunoassay of serum and urinary cortisol, Clin. Chim. Acta 63 (1975) 139–148.
[14] J. Cavanagh, W.J. Fairbrother, A.G. Palmer III, Mark Rance, N.J. Skelton, Protein NMR Spectroscopy: Principles and Practice, Second Edition, Elsevier Academic Press, Burlington, MA (USA), San Diego, CA (USA), and London (UK), 2007.
[15] H. Wang, Y. He, K.T. Hsu, J.F. Magliocca, J. Storch, R.E. Stark, 1H, ^{15}N and ^{13}C resonance assignments and secondary structure of apo liver fatty acid-binding protein, J. Biomol. NMR 12 (1998) 197–199.
[16] Y. He, X. Yang, H. Wang, R. Estephan, F. Francis, S. Kodukula, J. Storch, R.E. Stark, Solution-state molecular structure of apo and oleate-liganded liver fatty acid-binding protein, Biochemistry 46 (2007) 12543–12556.
[17] F. Delaglio, S. Grzesiek, G.W. Vuister, G. Zhu, J. Pfeifer, A. Bax, NMRPipe: a multidimensional spectral processing system based on UNIX pipes, J. Biomol. NMR 6 (1995) 277–293.
[18] B.A. Johnson, R.A. Blevins, NMR view: a computer program for the visualization and analysis ofNMR data, J. Biomol. NMR 4 (1994) 603–614.
[19] K.-T. Hsu, J. Storch, Fatty acid transfer from liver and intestinal fatty acid-binding proteins to membranes occurs by different mechanisms, J. Biol. Chem. 271 (1996) 13317–13323.
[20] T. Velkov, M.L. Lim, B. Capuano, R. Prankerd, A protocol for the combined sub-

fractionation and delipidation of lipid binding proteins using hydrophobic interaction chromatography, J. Chromatogr. B 867 (2008) 238–246.

[21] J. Cai, C. Lücke, Z. Chen, Y. Qiao, E. Klimtchuk, J.A. Hamilton, Solution structure and backbone dynamics of human liver fatty acid binding protein: fatty acid binding revisited, Biophys. J. 102 (2012) 2585–2594.

[22] A. Frolov, T.-H. Cho, E.J. Murphy, F. Schroeder, Isoforms of rat liver fatty acid binding protein differ in structure and affinity for fatty acids and fatty acyl CoAs, Biochemistry 36 (1997) 6545–6555.

[23] A. Gericke, E.R. Smith, D.J. Moore, R. Mendelsohn, J. Storch, Adipocyte fatty acid-binding protein: interaction with phospholipid membranes and thermal stability studied by FTIR spectroscopy, Biochemistry 36 (1997) 8311–8317.

[24] M.E. Hodsdon, J.W. Ponder, D.P. Cistola, The NMR solution structure of intestinal fatty acid-binding protein complexed with palmitate: application of a novel distance geometry algorithm, J. Mol. Biol. 264 (1996) 585–602.

[25] K.L. Constantine, M.S. Friedrichs, M. Wittekind, H. Jamil, C.-H. Chu, R.A. Parker, V. Goldfarb, L. Mueller, B.T. Farmer, Backbone and side chain dynamics of uncomplexed human adipocyte and muscle fatty acid-binding proteins, Biochemistry 37 (1998) 7965–7980.

[26] E. Marr, M. Tardie, M. Carty, T. Brown Phillips, I.-K. Wang, W. Soeller, X. Qiu, G. Karam, Expression, purification, crystallization and structure of human adipocyte lipid-binding protein (aP2), Acta Crystallogr. Sect. F: Struct. Biol. Cryst. Commun. 62 (2006) 1058–1060.

[27] L.E. Kay, Pulsed field gradient multi-dimensional NMR methods for the study of protein structure and dynamics in solution, Progress. Biophys. Mol. Biol. 63 (1995) 277–299.

[28] V. Kanelis, J.D. Forman-Kay, L.E. Kay, Multidimensional NMR methods for protein structure determination, IUBMB Life 52 (2001) 291–302.

[29] S.H. Rizk, Molecular Interactions of Adipocyte Fatty Acid-binding Protein with Activating and Non-activating Ligands: Protein Oligomerization and Ligand Binding Sites, City University of New York, New York, NY (USA), 2013.

[30] G.A. Petsko, D. Ringe, Protein Structure and Function, New Science Press, London (UK), 2004.

[31] F.A. Mulder, D. Schipper, R. Bott, R. Boelens, Altered flexibility in the substrate-binding site of related native and engineered high-alkaline Bacillus subtilisins, J. Mol. Biol. 292 (1999) 111–123.

[32] L. Kay, P. Keifer, T. Saarinen, Pure absorption gradient enhanced heteronuclear single quantum correlation spectroscopy with improved sensitivity, J. Am. Chem. Soc. 114 (1992) 10663–10665.

[33] D.S. Wishart, C.G. Bigam, J. Yao, F. Abildgaard, H.J. Dyson, E. Oldfield, J.L. Markley, B.D. Sykes, ^{1}H, ^{13}C and ^{15}N chemical shift referencing in biomolecular NMR, J. Biomol. NMR 6 (1995) 135–140.

[34] T. van der Wijk, J. Overvoorde, J. den Hertog, H_2O_2-induced intermolecular disulfide bond formation between receptor protein-tyrosine phosphatases, J. Biol. Chem. 279 (2004) 44355–44361.

[35] Y. Diao, W. Liu, C.C. Wong, X. Wang, K. Lee, P.-y. Cheung, L. Pan, T. Xu, J. Han, J.R. Yates, Oxidation-induced intramolecular disulfide bond inactivates mitogen-activated protein kinase kinase 6 by inhibiting ATP binding, Proc. Natl. Acad. Sci. USA 107 (2010) 20974–20979.

[36] G.V. Richieri, R.T. Ogata, A.M. Kleinfeld, Equilibrium constants for the binding of fatty acids with fatty acid-binding proteins from adipocyte, intestine, heart, and liver measured with the fluorescent probe ADIFAB, J. Biol. Chem. 269 (1994) 23918–23930.

[37] F. Ding, Q.-q. Li, L. Li, C. Gan, X. Yuan, H. Gou, H. He, C.-c. Han, J.-w. Wang, Isolation, culture and differentiation of duck (*Anas platyrhynchos*) preadipocytes, Cytotechnology 67 (2015) 773–781.

[38] D.R. Tocher, Metabolism and functions of lipids and fatty acids in teleost fish, Rev. Fish. Sci. 11 (2003) 107–184.

[39] Q. Wu, P. Andolfatto, N.H. Haunerland, Cloning and sequence of the gene encoding the muscle fatty acid binding protein from the desert locust, *Schistocerca gregaria*, Insect Biochem. Mol. Biol. 31 (2001) 553–562.

[40] W. Shepard, A. Haouz, M. Graña, A. Buschiazzo, J.-M. Betton, S.T. Cole, P.M. Alzari, The crystal structure of Rv0813c from Mycobacterium tuberculosis reveals a new family of fatty acid-binding protein-like proteins in bacteria, J. Bacteriol. 189 (2007) 1899–1904.

[41] S. Odani, Y. Namba, A. Ishii, T. Ono, H. Fujii, Disulfide bonds in rat cutaneous fatty acid-binding protein, J. Biochem. 128 (2000) 355–361.